

Dielectric properties of partially disordered lanthanum-modified lead zirconate titanate relaxor ferroelectrics

Boris Vodopivec,* Cene Filipič, Adrijan Levstik, Janez Holc, and Zdravko Kutnjak
Jožef Stefan Institute, P.O. Box 3000, 1001 Ljubljana, Slovenia

Horst Beige

Fachbereich Physik, Martin-Luther-Universität Halle-Wittenberg, 06108 Halle, Friedman-Bach-Platz 6, Germany

(Received 27 October 2003; published 23 June 2004)

Linear and third-order nonlinear dielectric susceptibilities and the dielectric polarization were measured in 6.5/65/35 lanthanum lead zirconate titanate (PLZT) hot-pressed ceramics. On cooling linear dielectric data show a transition from an ergodic to a nonergodic relaxor phase, while, on heating, a ferroelectric to ergodic relaxor phase transition appears. The third-order dielectric response is reminiscent of an ergodic to nonergodic relaxor phase transition. Below the Vogel-Fulcher temperature, at which the longest relaxation time diverges, spontaneous polarization exists, which indicates the possibility that the sample breaks up at low temperatures into relaxor glasslike and ferroelectric order-dominated regions at nonzero transition temperatures. Additional measurements of the quasistatic field-cooled-field-heated dielectric susceptibilities revealed an electric-field-temperature phase diagram, which confirmed the coexistence of both phases. The dielectric susceptibility at various bias electrical fields, obtained from polarization data, revealed a field-induced transformation between the disordered state and ordered ferroelectric state. The results were analyzed in the framework of the spherical random-bond-random-field model.

DOI: 10.1103/PhysRevB.69.224208

PACS number(s): 77.84.Dy, 77.22.Gm, 77.80.Bh

I. INTRODUCTION

Lanthanum doped lead zirconate titanate ceramics $\text{Pb}_{1-x}\text{La}_x(\text{Zr}_y\text{Ti}_{1-y})_{1-x/4}\text{O}_3$ (PLZT), with La content varying between 4 and 12 at.%, belong to the ferroelectric relaxor systems.¹ Between 4 and 7 at.%, the macroscopic properties change from normal ferroelectric to relaxor-ferroelectrics with increasing La content. For lanthanum concentrations above 7 at.%, these materials show a shift of the frequency peak maximum of the frequency dependent dielectric permittivity with decreasing temperature, the absence of any macro-symmetry changes, a characteristic slowing of dynamics according to the Vogel-Fulcher law, and a strong deviation from Curie-Weiss behavior.²⁻⁶

The formation of ferroelectric domains is strongly inhibited as the La content increases and a broad diffuse relaxor-like dielectric maximum also appears. Substitution of Pb^{2+} ions by La^{3+} ions creates vacancies in the A site of the perovskite ABO_3 structured ferroelectric PLZT ceramics and this is believed to break the long-range Coulomb interaction in the lattice. Between ferroelectrically active oxygen octahedrals containing B-site cations this interaction drives the formation of spontaneous polarization below T_c . Above a critical (>7 at.%) La content, the decoupling might be expected to be sufficiently strong to prevent spontaneous formation of a long-range ferroelectric state with micron-sized domains. Instead, a state with locally polarized regions on a nanometer scale is observed.⁷ It is therefore commonly recognized that all relaxor materials are highly inhomogeneous.^{2,3,8}

Polar nanodomain region results because of the above-mentioned fluctuation of composition and the appearance of lattice defects due to the method of their preparation (powder

sintering for PLZT materials), which favors chemical heterogeneity and residual stress.¹ In relaxorlike materials it is believed that correlations between polar nanodomains and subsequent freezing of polarization fluctuations into a state with glasslike characteristics at lower temperatures control the observed relaxor behavior.^{3,4,9,10} These nanopolar regions behave like spins “feeling” local electric random fields and interacting via random bonds.^{7,11}

The ferroelectric phase can only be stabilized in these glassy relaxor systems by cooling the system with applied electrical fields of values higher than the critical electrical field E_C , as was shown recently for $x/65/35$ PLZT relaxors ($7 < x < 12$),^{4,11,12} or by mechanical stress.^{8,12} An external electrical field can overcome the random local fields in such a way that a normal ferroelectric phase may be induced. This transition is often referred to in the literature as the field-induced micro- to macrodomain transition.² Thus, when an electric field is applied, nanodomains will grow in size and merge to form large polar regions, which results in macrodomains.¹³

It was shown that in (6–7)/65/35 PLZT ceramics cooled in zero electric bias field at low temperatures, regions dominated by both ferroelectric and glassy relaxor states could be formed. Optical and electrical measurements reported the coexistence of micro-sized ferroelectric domains and also nano-sized glassy polar regions.¹⁴⁻¹⁶ At room temperature the sizes of ferroelectric and glassy polar regions in (6–7)/65/35 PLZT are estimated to be 1–3 μm and approximately 10 nm, respectively.^{14,16}

While most earlier results were either focused on the limit of low electrical fields¹⁷ or on the samples well above 6 at.% La concentration, i.e., for pure glasslike systems, we have investigated the dielectric properties of the limiting system

between the ferroelectric dominated and glassy dominated La concentrations by linear and nonlinear dielectric experiments. Both point to the coexistence of ferroelectric and relaxor phases, in the absence of external bias electrical field. In addition, the electric-field–temperature (E – T) phase diagram was determined by quasistatic measurements of the field-cooled–field-heated (FC/FH) dielectric susceptibilities, which confirmed the coexistence of both phases.

II. EXPERIMENTAL PROCEDURES

PLZT samples were prepared by a mixed oxide method starting from high-purity oxides (>99.9 at. %). After being hot pressed at 1420 K for 2 h in PbO excess environment, gold electrodes were sputtered onto the sample by the evaporation technique. Measurements were made on three 6.5/65/35 PLZT ceramic samples with thicknesses from 0.26 mm to 0.32 mm. Complex dielectric permittivity was measured using a Hewlett-Packard 4282A Precision LCR meter. The amplitude of the ac excitation voltage was 1 V. Measurements were performed on cooling and heating the sample between 453 K and 295 K, typically with the rate of ± 60 K/h, in several dc bias electrical fields from 0 to 5 kV/cm and in the frequency range between 20 Hz and 1 MHz.

The temperature and the dc field dependence of the effective quasistatic field-cooled (FC) dielectric susceptibility $\chi_{FC} = P_{FC}(E, T)/E$ was determined by cooling (FC) and subsequently heating (FH) an annealed sample, in a dc bias electrical field E , while the corresponding polarization charge was measured by the Keithley 617 programmable electrometer.¹⁸

Since it is well known that history-dependent effects play an important role in relaxor systems, the samples were annealed at 453 K for 1 h before each measurement, in order to ensure identical conditions for all measurements and to eliminate the effects of previous treatments.^{4,19}

A. Results and analysis

The temperature dependence of the dielectric loss factor $\tan(\delta) = \epsilon''/\epsilon'$, obtained on cooling and heating the sample, is shown in Figs. 1(a) and 1(b). Data taken on cooling differ from those obtained on heating the sample. While on cooling the sample from 458 K the dielectric loss factor shows continuous evolution [Fig. 1(a)]; on heating, this quantity exhibits a less discontinuous increase near 412 K [Fig. 1(b)].

It was reported that such behavior could be a consequence of a space charge field.¹⁶ In PLZT ceramics a space charge field is built up by the redistribution of the defects and/or space charge. This field is stabilized by coupling with the spontaneous polarization. An internal field thus helps to induce the ferroelectric state.¹⁶ By heating the sample to 473 K the space charge and the internal field completely disappear. Therefore on cooling, the internal field is much smaller than on heating, and consequently a difference in $\epsilon^*(T)$ between the cooling and heating cycles appears. This means that the low temperature state, which was reached immediately after cooling the sample, is not yet in equilibrium and conforms more to the relaxor glassy state. On further cooling the part

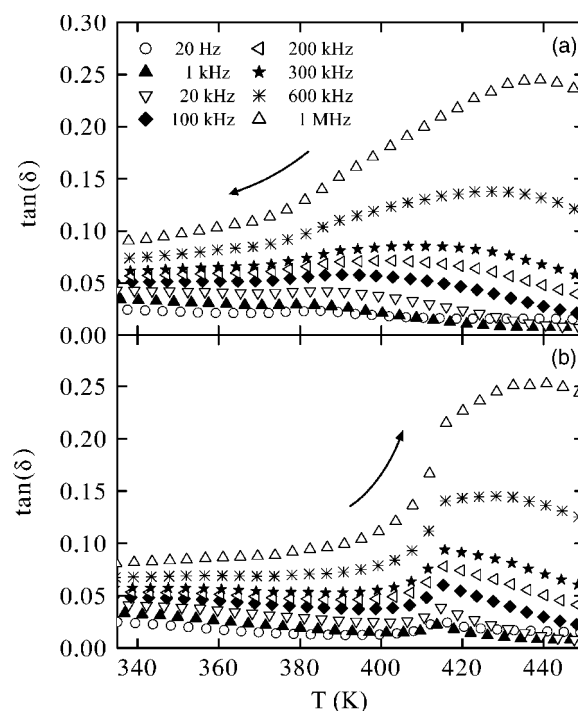


FIG. 1. The dielectric loss factor $\tan(\delta)$ as a function of temperature for several measurement frequencies taken on cooling (a) and heating (b). Both cooling and heating runs were taken in zero bias electric field.

of the sample slowly converts to the long-range ferroelectric state as the space charge field builds up after the redistribution of the defects and space charges has taken place. The redistribution of the defects and space charges via diffusion have support in the aging effects observed in PLZT system, which occur below some particular temperature (ca. 420–470 K in PLZT ceramics, see for instance Ref. 20 and references therein). As the diffusion of the defects is rather slow at lower temperatures, so are also aging effects and conversion to long-range ferroelectric state, which both could take hours or days. However, the space charge mechanism should only be looked as and an auxiliary mechanism that helps to convert the system to the ferroelectric order. This conversion might account for the rather smooth change in the slope in $\tan(\delta)(T)$ data near 385 K [see Fig. 1(a)].

It appears that the above conversion to a long-range ferroelectric state is rather sluggish, so that immediately after cooling most of the sample ends up actually in a state similar to the relaxor glassy state. The glassy nature of the state reached immediately after cooling is also evident from the analysis of the freezing dynamics. The temperature dependence of the characteristic relaxation frequency obtained from the temperatures corresponding to the diffuse $\epsilon''(T)$ peaks obtained on cooling obeys the Vogel-Fulcher ansatz

$$f = f_0 \exp[-E_a/(T - T_F)], \quad (1)$$

with $E_a = 0.039$ eV, $f_0 = 132$ MHz, and the freezing temperature $T_F = 360 \pm 2$ K. Such behavior is characteristic for a freezing process from an ergodic to a nonergodic relaxor phase.^{3,17} The observed dynamics are similar to the glassy

dynamics reported for the pure relaxor in zero external bias field, 9/65/35 PLZT ceramic,⁴ which does not show ferroelectric long-range order in zero electric bias fields. Here the nanoclusters interact through random bonds in the environment of random fields.

In 6.5/65/35 PLZT ceramics, due to the gradual growth of the polar nanoregions in the relaxor phase on cooling and due to the decreasing thermally activated reorientation of the polarization in nanoregions, the correlation between the nanoregions increases. Consequently the size of the polar regions also increases with time.¹⁶ Thus a similar time dependence was observed^{21,22} in measurements of the ferroelectric hysteresis loop at room temperature. However, the predominant broad glassy relaxor dielectric response which persists in the whole temperature range indicate that the ferroelectric phase is probably stabilized in only a very small fraction of the sample. Moreover, Dai *et al.* reported¹⁵ the detection of both polar nanocluster state and micrometer-sized ferroelectric domain state, using x-ray diffraction, i.e., the coexistence of both relaxor and ferroelectric phases at room temperature. Indeed it seems that the system properties based on our data conforms to the case of the relatively spatially large correlated ferroelectric regions in the presence of a large volume of unconverted glassy polar nanoclusters.

In contrast to the response obtained on cooling, a rather sharp change of slope in the dielectric loss factor is seen on heating at 412 K [Fig. 1(b)]. The sharpness of the change of slope and the transition temperature hysteresis are indications of the weakly first order nature of the transition in which the ferroelectric part of the samples converts to the ergodic relaxor state.^{12,23} Recent investigations, involving dielectric hysteresis and x-ray diffraction measurements, support the above idea that a spontaneous ferroelectric to ergodic relaxor phase transition takes place at this temperature.^{15,16} The space charge field which helped to induce the ferroelectric state gradually disappears with increasing temperature, thus allowing the thermal fluctuations to destroy the long-range correlations between micro domains. A broad dielectric maximum is seen at 445 K in the real and imaginary part of the complex permittivity. This maximum was shown to be purely of dynamic origin.^{3,4} Whenever the longest relaxation time of the system exceeds the experimental time scale, the measured dielectric constant starts to deviate from the static response, resulting in a broad peak at a temperature which depends on the measuring frequency. An additional indication of the sluggish conversion from the relaxor to the ferroelectric phase is given by the dynamic measurements of the third harmonic nonlinear dielectric response $|\epsilon_3|$.²⁴

It was shown recently that the static dielectric nonlinearity

$$|a_3| = |\chi_3|/\chi_1^4 \quad (2)$$

in zero bias electric field (ZFC) could reveal the universality class of the system under study.^{4,25,26} According to Kutnjak *et al.*,⁴ $|a_3|$ should decrease continuously through the glassy relaxor to ferroelectric phase transition or rather steeply increase in the case of the ergodic relaxor to nonergodic relaxor phase transition. It was shown recently that a different response should be expected in these systems in the case of

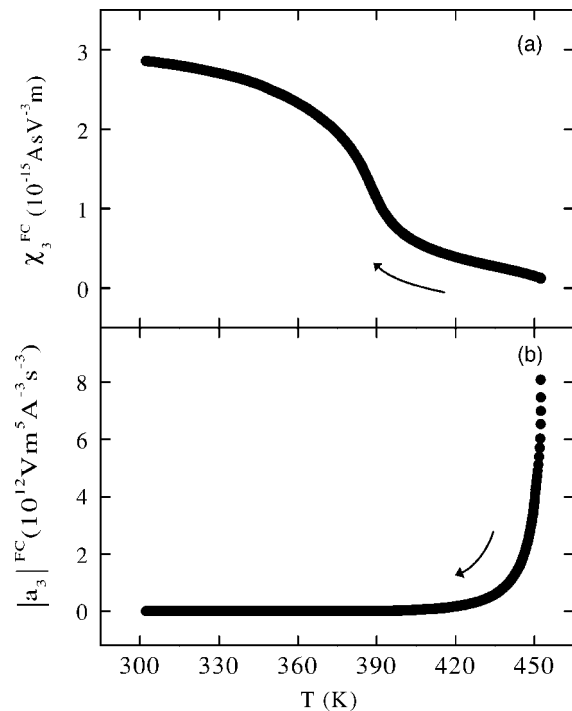


FIG. 2. (a) The total static third order nonlinear dielectric susceptibility χ_3 as a function of temperature and (b) the temperature dependence of the quasistatic nonlinearity $|a_3|$ measured on cooling.

FC measurements.²⁷ Thus, due to the nearly critical nature of these systems, an external field strongly modulates inter-cluster coupling which strongly influences the temperature dependence of $|a_3|^{FC}$ obtained in an FC experiment.^{27,28} In order to verify the temperature dependence of a_3^{FC} , the dielectric polarization P_{FC} was measured at various static external fields E . The quasistatic third order nonlinear dielectric coefficient χ_3^{FC} [see Fig. 2(a)] was then calculated from

$$\chi_3^{FC} = \frac{\chi_{FC}(E_2) - \chi_{FC}(E_1)}{E_2^2 - E_1^2}, \quad (3)$$

where $E_1 = 3.5$ kV/cm and $E_2 = 13.8$ kV/cm. In contrast to the dynamic results²⁴ the $a_3^{FC}(T)$ shown in Fig. 2(b) resembles more the response expected for ferroelectrics as would be expected in an applied bias electric field.²⁷ It should be mentioned that both quantities χ_3^{FC} and a_3^{FC} shown in Figs. 2(a) and 2(b) exceeds previously published values obtained in glassy relaxor systems such as PMN single crystal and 9/65/35 PLZT ceramics^{27,28} by a three orders of magnitude. The reason for this could be the existence of larger ferroelectric domains at low temperatures, which significantly contribute to the dielectric nonlinearity via the domain wall motion mechanism. The dynamic²⁴ and quasistatic nonlinear results show that the aforementioned relaxor materials exhibit a class of nonlinear behavior different from that found in dipolar glasses or ferroelectric materials.^{27,28}

Quasistatic measurements of the FC/FH effective dielectric polarization response at several different dc fields obtained with 6.5/65/35 PLZT ceramics are shown in Fig. 3. Results are very similar to those obtained previously at simi-

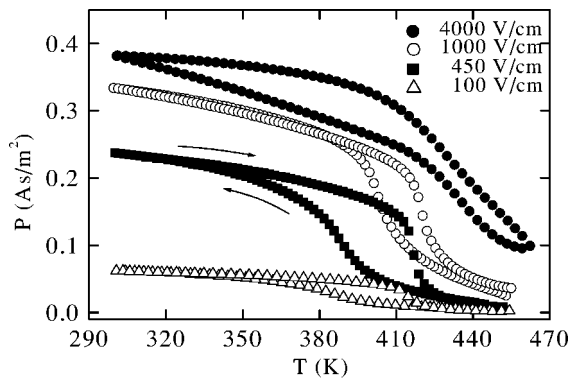


FIG. 3. Temperature dependence of FC/FH effective dielectric polarization P , measured at different bias external fields. Arrows indicate a heating and cooling run.

lar fields on glassy ferroelectric-relaxor (8-9)/65/35 PLZT ceramics^{4,9,29} and on PMN relaxor.²⁷ In particular, the FC dielectric susceptibility increases very sharply with decreasing temperature and nearly saturates at lower temperatures. This rather sharp increase corresponds to the relaxor-to-ferroelectric conversion, which takes place even in a zero-field cooled run. It can be seen, as previously described, as a steplike anomaly in the dielectric loss on heating [Fig. 1(b)].

Again hysteresis is observed (Fig. 3) between FC and FH quasistatic dielectric polarizations in the temperature range around the ferroelectric transition.

Figure 4 shows the field dependence of the FC quasistatic dielectric polarization deduced from different FC scans (Fig. 3) obtained at various dc electrical fields.²⁹ After an approximately linear regime, the polarization saturates in an almost field-independent plateau. This plateau corresponds to the spontaneous polarization P_S , which reaches a value of nearly 0.37 As/m^2 at low temperatures.

From polarization data (Fig. 4), a spontaneous polarization P_S at different temperatures can be obtained (see Fig. 5). A tentative fit to the critical ansatz $P_S = (T - T_c)^\beta$ gives rather small value of the $\beta = 0.15$ (see solid line in Fig. 5). This can be explained as an artifact of the smeared weakly first ordered transition, which results in a steeper rise of the P_S , thus effectively suppressing the critical exponent β .

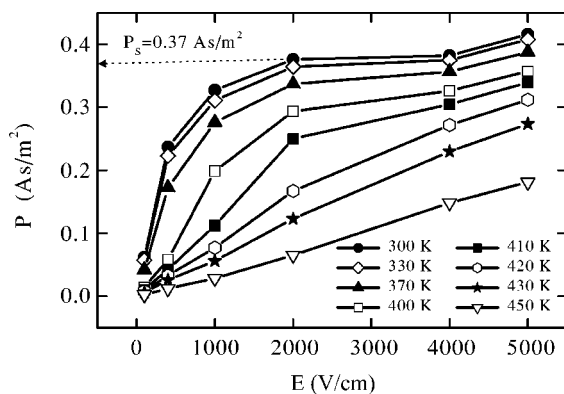


FIG. 4. Dielectric polarization measured on cooling at different temperatures and different electrical fields. The value of spontaneous polarization at 300 K is also shown.

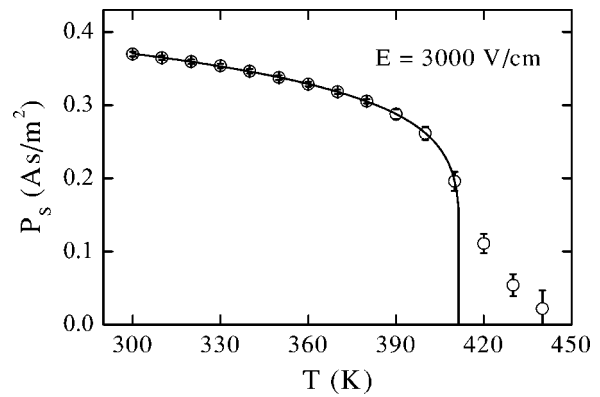


FIG. 5. Spontaneous polarization as a function of temperature at $E = 3 \text{ kV/cm}$. The solid line represents a tentative fit of measured data to $P_S = (T - T_c)^\beta$, where $T_c = 412 \text{ K}$ and $\beta = 0.15$.

It should also be noted that P_S vanishes at the same temperature at which the pyroelectric current exhibits a sharp peak (Fig. 6). The pyroelectric currents were calculated from the derivatives of the $P_{FC/FH}(T)$ data (Fig. 3). This allows determination of the ergodic relaxor to ferroelectric (T_c) transition temperatures from the temperature positions of the pyroelectric current peaks (Fig. 6).

From measurements of the spontaneous polarization a derivative corresponding to the effective susceptibility $\chi_1 = dP/dE$ was calculated at each measured value of bias electrical field and particular temperature. Subsequently each of these susceptibility values was drawn for each temperature at which they were calculated in order to obtain the susceptibility graph for different values of bias electrical fields. χ_1 so

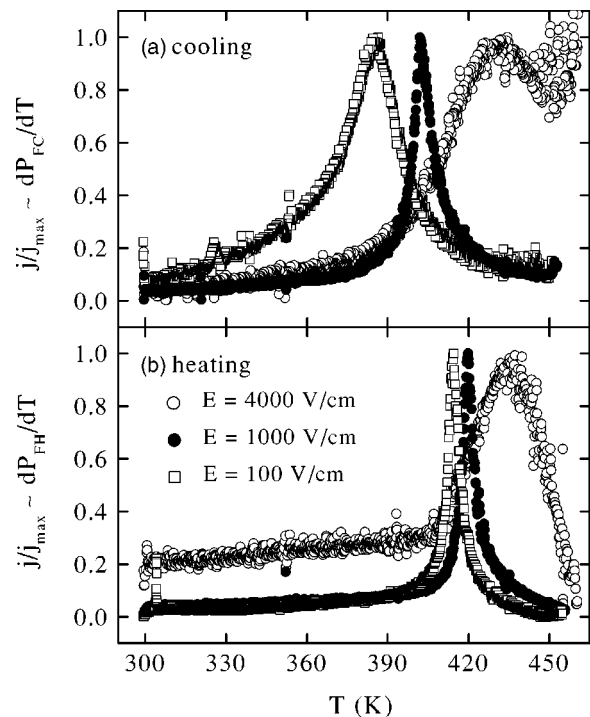


FIG. 6. Rescaled pyroelectric current peaks proportional to the dP/dT obtained at different bias external electrical fields for (a) cooling and (b) heating run.

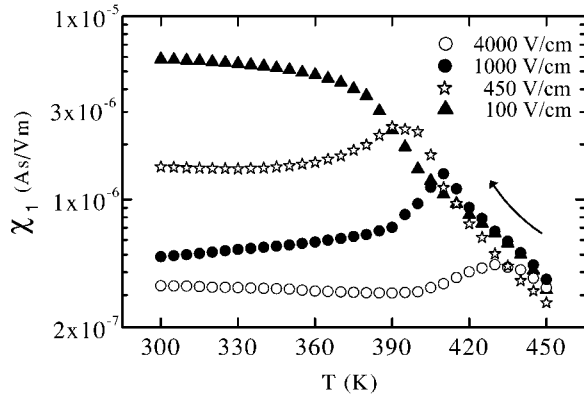


FIG. 7. Effective dielectric susceptibility as a function of temperature at various bias electrical fields, obtained from spontaneous polarization data on cooling.

obtained and presented in Fig. 7 resembles features typical of the inhomogeneous ferroelectric transition. In particular, the broad smeared peaks (Fig. 7) correspond to the smeared soft mode anomaly, typically observed at a ferroelectric transition. These peaks appear at the temperatures at which the pyroelectric current exhibits peak anomalies, that is, at the ferroelectric transition points at which the polarization exhibit strong changes.

Furthermore, the FC susceptibility curve corresponding to the particular value of the dc electric field saturates at lower temperatures, typically at rather larger plateau values, instead of decreasing back to small values similar to those above the peak anomaly. With the increasing dc electric field the peak anomalies become more pronounced while the low temperature plateau values decrease. This behavior is reminiscent of the domain wall motion effects typically observed in ferroelectrics which usually results in a strong deviation from the Curie-Weiss behavior or even saturation of susceptibility values below the ferroelectric transition temperature. This in turn agrees with the idea that, with increasing dc electric field, part of the sample becomes more and more ferroelectriclike with growing domains.

On the other hand, analysis of the frequency-dependent complex dielectric constant (Fig. 8) reveals that, in small bias electrical fields, part of the sample still freezes into the glasslike nonergodic relaxor state, even below the RF transition temperature. The freezing transition temperature T_F of this glassy relaxor state is shown as a function of the bias electric field in Fig. 9(b). Here, the temperature dependence of the characteristic relaxation frequency determined from the temperature positions of the diffuse imaginary dielectric peaks obtained at different bias electrical fields (inset to Fig. 8) obeys the Vogel-Fulcher ansatz [Eq. (1)] with the freezing temperature T_F now strongly dependent on the bias electric field. The susceptibility anomalies could also be used to establish the phase transition temperatures and thus the E - T phase diagram. In zero bias electric field the ferroelectric phase transition temperature was found to be 383 K on cooling and 413 K on heating, while on increasing the bias electric field, a nearly linear increase in ergodic relaxor to ferroelectric (RF) phase transition temperature was observed (+11 K per 1 kV/cm on cooling) (Fig. 9).

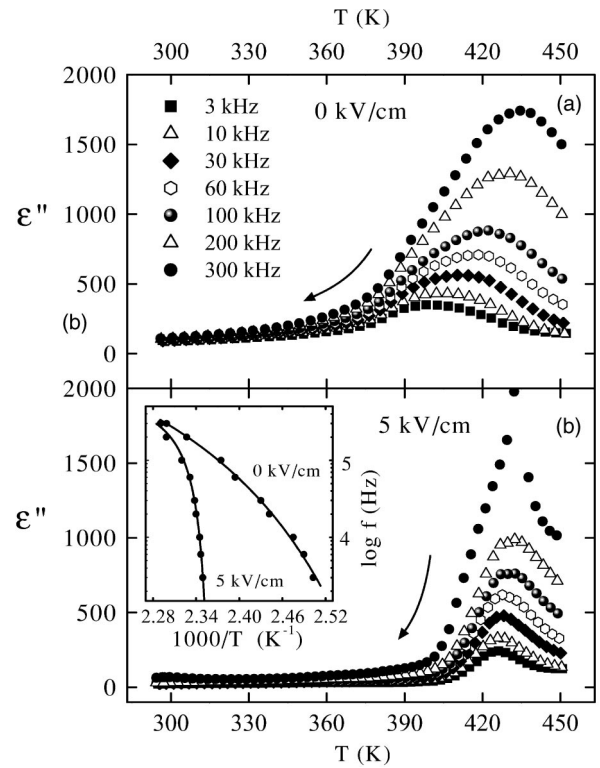


FIG. 8. Imaginary part of the linear dielectric constant as a function of the temperature on cooling in a zero bias electric field (a) and in $E=5$ kV/cm (b). The inset shows the characteristic relaxation frequency as a function of the inverse temperature in zero bias electric field and in $E=5$ kV/cm.

Furthermore, temperature positions of the diffuse peaks of the imaginary part of the dielectric constant become almost frequency independent, as one would expect for the critical slowing down in the vicinity of the ferroelectric phase transition. This is reflected in very steep curves for the temperature dependence of the characteristic relaxation frequency [inset to Fig. 8(b)], which become more and more activated-like as more and more of the sample converts to the ordered ferroelectric state with the increasing external bias electrical field. It appears that, at much larger electric bias field, a ferroelectric state would be dominant, as relaxor polar nanoregions would tend to convert into ferroelectric micron-sized domains. In this case, a sharper first order ferroelectric phase transition exhibiting a divergence in the dielectric response should be seen and an additional critical-slowing-down anomaly should appear in the Arrhenius temperature dependence of the characteristic relaxation frequency.

III. THEORY

It has been shown that the SRBRF model^{7,30} can be used to describe the transition from ergodic to nonergodic relaxor phase or even the field-induced transition from ergodic relaxor phase to ferroelectric phase.^{11,12} The Hamiltonian is written in the form

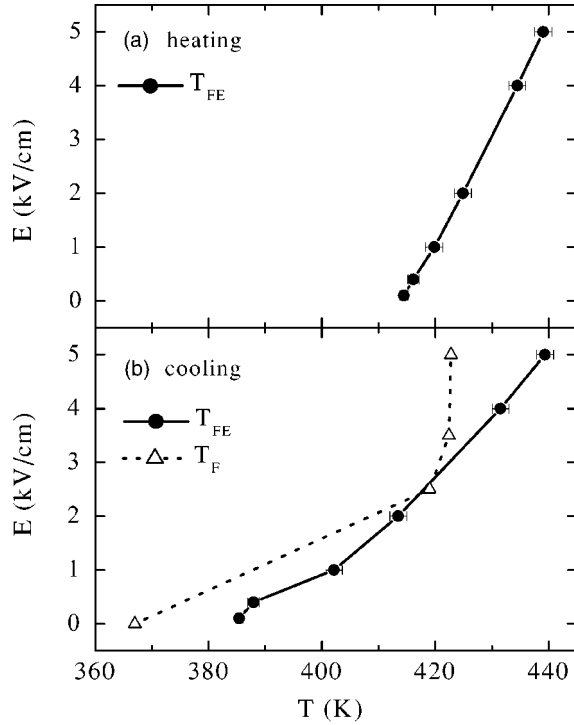


FIG. 9. (a) Relaxor to ferroelectric transition temperature T_{FE} on heating and (b) on cooling together with freezing transition temperature T_F as a function of the electric field.

$$H = -\frac{1}{2} \sum_{ij} J_{ij} S_i S_j - \sum_i h_i S_i - \varphi g \sum_i E S_i, \quad (4)$$

where S_i is a scalar order parameter field, related to the dipole moment of the i th polar cluster. Random bonds J_{ij} are characterized by the mean value of the coupling J_0/N and the variance J^2/N and random fields h_i are characterized by the variance Δ . Electric field, E , influence is scaled with average cluster dipole moment g , and φ is the local field factor. Calculation of the average free energy yields equations for the spherical glass order parameter q and polarization P in the form^{12,27,28}

$$q = \beta^2 J^2 (q + \Delta/J^2)(1 - q)^2 + P^2, \quad (5)$$

$$P = \beta(1 - q)(J_0 P + \varphi g E). \quad (6)$$

The above dimensionless equations could be rescaled by introducing $\tilde{P} = \rho P$ so that standard metric units apply, i.e., \tilde{P} ,

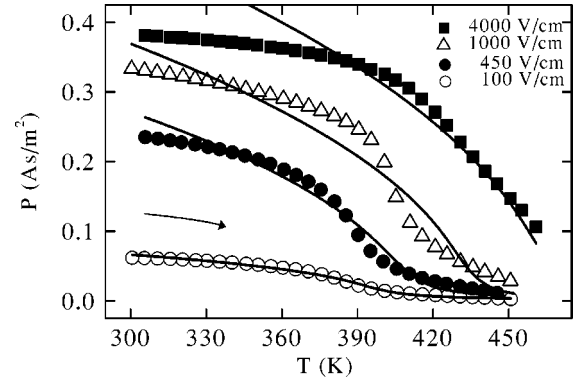


FIG. 10. FC dielectric polarization as a function of temperature at various bias electrical fields. Solid lines represent fits to Eqs. (5)–(7).

$\beta = 1/kT$, J , are given in As/m², 1/J, J, respectively. Here parameter ρ is related to the sample-dependent volume density of dipoles and translates the dimensionless P to the macroscopic polarization \tilde{P} . The ferroelectric phase exists only if $J_0 > J_{0c}$, where the critical value is given^{27,30} by $J_{0c} = \sqrt{J^2 + \Delta}$. In order to describe the change from a glassy phase to a ferroelectric one in an electric field E , the field-dependent parameter $J_0(E)$ was recently introduced¹²

$$J_0 = \sqrt{J^2 + \Delta} + \gamma E^2, \quad (7)$$

which provided rather well a quantitative phenomenological description of the E – T phase diagram of relaxor ferroelectrics.¹² Here γ is a free parameter.

Nonlinear least square fits of the above equations to our data yield $q(E, T)$ and $P(E, T)$ (solid lines in Fig. 10), with typical free fitting parameters (see Table I).

It should be noted that the SRBRF fits are quantitatively well at lower electrical fields, while at higher electrical fields deviations start to appear at lower temperatures and consequently susceptibility peaks start to deviate from RF temperatures as an artifact of the poor fit. These low temperature deviations could be due to the fact that at higher electrical fields the conversion to the ferroelectric phase is more complex than could be described by our model and perhaps additional higher order terms for electrical field influence should be incorporated. The effects of impurities and pinning effects could also play an important role not incorporated in our model.

TABLE I. Fit parameters for Eqs. (5)–(7) obtained from nonlinear least square fits to dielectric polarization data (see Fig. 10).

E (V/cm)	100	450	1000	4000
J/k (K)	398	400	406	419
Δ/J^2	0.0009	0.034	0.16	0.24
γ/k (m ² K/V ²)	9.8×10^{-10}	2.4×10^{-8}	1.0×10^{-8}	8.9×10^{-10}
$\varphi g/k$ (mK/V)	1.4×10^{-5}	3.7×10^{-6}	3.7×10^{-7}	3.4×10^{-7}
ρ (As/m ²)	1.15	1.16	1.15	1.10

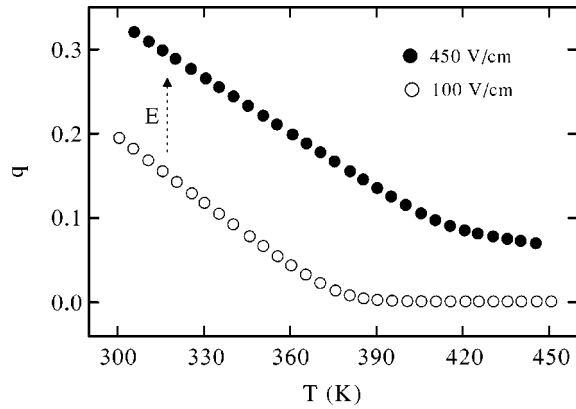


FIG. 11. Spherical glass order parameter obtained from polarization measurements by using Eqs. (5) and (6) as a function of temperature at two different bias electrical fields.

The experimental behavior of the spherical glass order parameter $q(E, T)$ so determined is shown in Fig. 11. Its value gradually approaches zero with increasing temperature, in accordance with SRBRF model predictions in the presence of weak random fields. Increasing the electric bias field increases the phase transition temperatures (see $E-T$ phase diagram in Fig. 9) and enhances ordering effects, hence the larger values of q at all temperatures. The dielectric susceptibility

$$\chi_1^{FC}(E, T) = \partial P / \partial E, \quad (8)$$

was calculated using Eqs. (5) and (7) and the fitting parameters in Table I (see Fig. 12).

Calculated susceptibility curves at larger bias electrical fields in Fig. 12 qualitatively resemble those obtained experimentally in Fig. 7, with the soft mode related susceptibility peaks which gradually shift toward higher temperatures as the RF transition temperature increases with increasing bias field, indicating that the SRBRF model can indeed qualitatively account for the main features observed at the RF transition.

Figure 13 shows χ_3^{FC} and a_3^{FC} calculated from²⁸

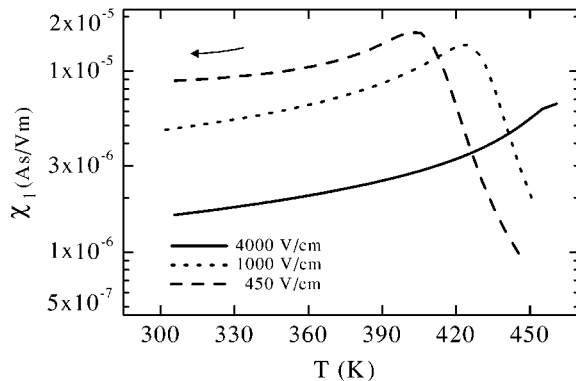


FIG. 12. Dielectric susceptibility as a function of temperature at various bias electrical fields (compare to Fig. 7) calculated from Eq. (8) by using parameters obtained from SRBRF fits of spontaneous polarization (see Fig. 10).

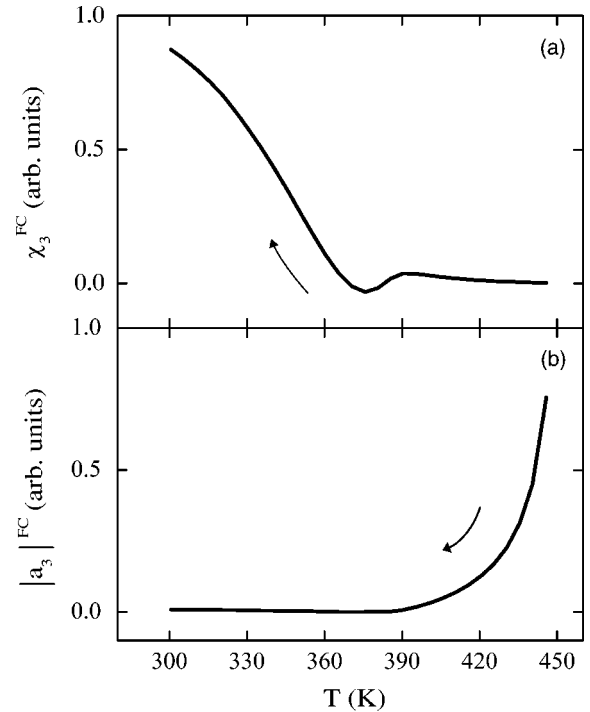


FIG. 13. Calculated temperature dependence of (a) $\chi_3(T)$ and (b) $a_3(T)$ on cooling obtained from Eqs. (9) and (2) using parameters in Table I.

$$\chi_3(E, T) = -(1/6) \partial^3 P / \partial E^3, \quad (9)$$

and Eq. (2), by using the fitting parameters in Table I.

Both calculated quantities χ_3^{FC} and a_3^{FC} in Fig. 13 agree qualitatively with the observed behavior of χ_3^{FC} and a_3^{FC} [see Figs. 2(a) and 2(b)].

IV. CONCLUSIONS

Measurements of the linear and nonlinear dielectric response show that in 6.5/65/35 PLZT hot-pressed ceramics, on cooling in zero bias electric field, the ergodic to nonergodic relaxor phase transition occurs at 360 ± 2 K. A slow conversion from the relaxor state to the microdomain ferroelectric state takes place at low temperatures. As a consequence, the spontaneous transition from the ferroelectric to the ergodic relaxor phase could be monitored at 412 K on heating the sample. However, the presence of the soft mode anomaly in the linear dielectric susceptibility and the slowing dynamics according to the Vogel-Fulcher law, as well as the temperature dependence of the dielectric nonlinearity $|a_3|$, show that both relaxor glasslike and ferroelectric order dominated regions coexist at low temperatures.

The $E-T$ phase diagram, deduced from Vogel-Fulcher temperatures and pyroelectric current data, show for both relaxor and ferroelectric states increase of the transition temperatures with increasing bias electric field. The coexistence of multidomain states in PLZT 6.5/65/35 is most probably stabilized by a random distribution of local fields. Additional measurements of the complex dielectric constant and FC/FH quasistatic dielectric polarization in bias electrical field show

that nanoscale polar regions slowly grow with increasing bias field to the ordered ferroelectric microdomains.

The linear dielectric response at larger values of the bias electric field resembles a soft mode anomaly, similar to the response one would expect near the inhomogeneous ferroelectric transition. It is shown that the extended SRBRF model^{12,28} could provide rather well a qualitative description

of the electric-field-induced dielectric features including the E - T phase diagram.

ACKNOWLEDGMENT

This work was supported by the Slovenian Office of Science and Slovene-German Cooperation Project.

*Electronic address: boris.vodopivec@ijs.si

- ¹R. Farhi, M. E. Marssi, J. L. Dellis, J. C. Picot, and A. Morell, *Ferroelectrics* **176**, 99 (1996).
- ²D. Viehland, S. J. Jang, and L. E. Cross, *J. Appl. Phys.* **68**, 2916 (1990).
- ³A. Levstik, Z. Kutnjak, C. Filipič, and R. Pirc, *Phys. Rev. B* **57**, 11204 (1998).
- ⁴Z. Kutnjak, C. Filipič, R. Pirc, A. Levstik, R. Farhi, and M. E. Marssi, *Phys. Rev. B* **59**, 294 (1999).
- ⁵S. Kamba, V. Bovtun, J. Petzelt, I. Rychetsky, R. Mizaras, A. Brilingas, J. Banys, J. Grigas, and M. Kosec, *J. Phys.: Condens. Matter* **12**, 497 (2000).
- ⁶V. Bovtun, J. Petzelt, V. Porokhonsky, S. Kamba, and Y. Yakimenko, *J. Eur. Ceram. Soc.* **21**, 1307 (2001).
- ⁷R. Blinc, J. Dolinšek, A. Gregorovič, B. Zalar, C. Filipič, Z. Kutnjak, A. Levstik, and R. Pirc, *Phys. Rev. Lett.* **83**, 424 (1999).
- ⁸M. E. Marssi, R. Farhi, J. L. Dellis, M. D. Glinchuk, L. Seguin, and D. Viehland, *J. Appl. Phys.* **83**, 5371 (1998).
- ⁹D. Viehland, J. F. Li, S. J. Jang, L. E. Cross, and M. Wuttig, *Phys. Rev. B* **46**, 8013 (1992).
- ¹⁰E. V. Colla, E. Y. Koroleva, N. M. Okuneva, and S. B. Vakhru-shev, *Phys. Rev. Lett.* **74**, 1681 (1995).
- ¹¹V. Bobnar, Z. Kutnjak, and A. Levstik, *Appl. Phys. Lett.* **76**, 2773 (2000).
- ¹²V. Bobnar, Z. Kutnjak, R. Pirc, and A. Levstik, *Phys. Rev. B* **60**, 6420 (1999).
- ¹³U. Bottger, A. Biermann, and A. Arlt, *Ferroelectrics* **134**, 253 (1992).

- ¹⁴J. L. Dellis, M. E. Marssi, P. Tilloly, R. Farhi, and D. Viehland, *Ferroelectrics* **201**, 167 (1997).
- ¹⁵X. H. Dai, Z. Xu, and D. Viehland, *J. Am. Ceram. Soc.* **79**, 1957 (1996).
- ¹⁶A. Krumins, T. Shiosaki, and S. Koizumi, *Jpn. J. Appl. Phys., Part 1* **33**, 4940 (1994).
- ¹⁷X. H. Dai, Z. Xu, and D. Viehland, *Philos. Mag. B* **70**, 33 (1994).
- ¹⁸A. Levstik, C. Filipič, Z. Kutnjak, I. Levstik, R. Pirc, B. Tadić, and R. Blinc, *Phys. Rev. Lett.* **66**, 2368 (1991).
- ¹⁹A. Burkhanov and A. Shilnikov, *Ferroelectrics* **90**, 39 (1989).
- ²⁰Z. Kutnjak, C. Filipič, V. Bobnar, and A. Levstik, *Ferroelectrics* **240**, 273 (2000).
- ²¹Z. Xu, X. H. Dai, J. F. Li, and D. Viehland, *Appl. Phys. Lett.* **68**, 1628 (1996).
- ²²Q. Tan and D. Viehland, *Ferroelectrics* **209**, 589 (1998).
- ²³G. H. Haertling, *J. Am. Ceram. Soc.* **54**, 303 (1971).
- ²⁴C. Filipič, B. Vodopivec, J. Holc, A. Levstik, Z. Kutnjak, and H. Beige, *J. Eur. Ceram. Soc.* **24**, 1565 (2004).
- ²⁵V. Bobnar, Z. Kutnjak, R. Pirc, R. Blinc, and A. Levstik, *Phys. Rev. Lett.* **84**, 5892 (2000).
- ²⁶A. E. Glazounov and A. K. Tagantsev, *Phys. Rev. Lett.* **85**, 2192 (2000).
- ²⁷Z. Kutnjak, R. Pirc, and R. Blinc, *Appl. Phys. Lett.* **80**, 3162 (2002).
- ²⁸R. Pirc, R. Blinc, and Z. Kutnjak, *Phys. Rev. B* **65**, 214101 (2002).
- ²⁹Z. Kutnjak, C. Filipič, and A. Levstik, *J. Eur. Ceram. Soc.* **21**, 1313 (2001).
- ³⁰R. Pirc and R. Blinc, *Phys. Rev. B* **60**, 13470 (1999).